FeP Nanoparticles Film Grown on Carbon Cloth: An Ultrahighly Active 3D Hydrogen Evolution Cathode in Both Acidic and Neutral Solutions

ARTICLE *in* ACS APPLIED MATERIALS & INTERFACES · NOVEMBER 2014

Impact Factor: 6.72 · DOI: 10.1021/am5064684 · Source: PubMed

ACS APPLIED MATERIALS & INTERFACES

Letter

www.acsami.org

FeP Nanoparticles Film Grown on Carbon Cloth: An Ultrahighly Active 3D Hydrogen Evolution Cathode in Both Acidic and Neutral Solutions

Jingqi Tian,[†,‡] Qian Liu,[†] Yanhui Liang,[†] Zhicai Xing,[†] Abdullah M. Asiri,[§,∥] and Xuping Sun*[,†]

[†]State Key Lab of Electroanalytical Chemistry, Changchun Institute of Applied Chemistry, Chinese Academy of Sciences, Changchun 130022, Jilin China

[‡]Graduate School of the Chinese Academy of Sciences, Beijing 100039, China

[§]Chemistry Department, Faculty of Science, and [∥]Center of Excellence for Advanced Materials Research, King Abdulaziz University, Jeddah 21589, Saudi Arabia

Supporting Information

ABSTRACT: In this Letter, we demonstrate the direct growth of FeP nanoparticles film on carbon cloth (FeP/CC) through low-temperature phosphidation of its Fe_3O_4/CC precursor. Remarkably, when used as an integrated 3D hydrogen evolution cathode, this FeP/CC electrode exhibits ultrahigh catalytic activity comparable to commercial Pt/C and good stability in acidic media. This electrode also performs well in neutral solutions. This work offers us the most cost-effective and active 3D cathode toward electrochemical water splitting for large-scale hydrogen fuel production.

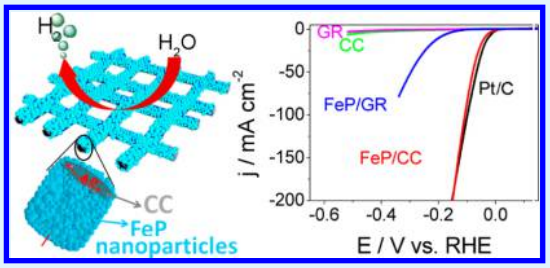

KEYWORDS: *FeP nanoparticles, 3D hydrogen evolution cathode, ultrahigh activity, water splitting, acidic and neutral solutions*

Hydrogen is an ideal clean and renewable energy carrier and is considered as one promising alternative to fossil fuels.[1] Efficient hydrogen generation by water splitting requires advanced electrocatalysts.[2] Pt-group metals are the most effective HER catalysts but suffer from high cost. Proton exchange membrane technology-based water electrolysis units need catalysts working under strongly acidic conditions.[3] These have stimulated considerable research into exploring acid-stable nonprecious metal alternatives made of earth-abundance elements. Among such catalysts, Mo-based compounds are a big family with great success, including sulfides, selenides, carbides, borides, nitrides,[4−6] etc. Microbial electrolysis cell, however, needs catalysts active at neutral pH.[7] It is thus highly desired to develop HER catalysts working efficiently in both acidic and neutral solutions but remains challenging.[8]

Transition metal phosphides are an important class of compounds with good electrical conductivity, and they have been widely used as catalysts for hydrodesulfurization and hydrodenitrogenation reactions as well as anode materials for Li-ion batteries.[9] Transition metal phosphides are recently emerged as an interesting new class of catalysts for the HER. Schaak and co-workers have developed Ni_2P and CoP hollow nanoparticles as efficient HER catalysts in acidic media, but several organic solvents are involved for catalyst preparation.[10] We have developed a facile strategy for preparing CoP nanocrystals decorated carbon nanotube nanohybrid (CoP/CNT) as a highly active acid-stable HER catalyst through low-temperature phosphidation of its Co_3O_4/CNT precursor.[11] All these catalysts are usually required to be effectively immobilized on current collectors using a polymer binder prior to electrochemical tests. The polymer binder, however, generally increases the series resistance[12] and may block active sites and inhibit diffusion, leading to reduced catalytic activity.[13] These issues can be solved by directly growing the active phases on current collectors.[8,14,15]

Iron is the cheapest and one of the most abundant of all transition metals while carbon is the most abundant element in the world. Xu et al. have developed FeP nanosheets as a HER catalyst in acidic solutions, but this catalyst needs a large overpotential (η) of ∼240 mV to afford current density of 10 mA cm^{-2} and still suffers from the use of several organic solvents for preparation.[16] Following our recently developed low-temperature phosphidation method, Zhang et al. have developed FeP nanoparticles grown on graphene sheet (FeP-GS) from its Fe_3O_4-GS precursor and this catalyst needs overpotential of 123 mV to drive current density of 10 mA cm^{-2}.[17] One-dimensional (1D) FeP arrays have also been developed on Ti plate as an efficient hydrogen evolution cathode.[18] A rough estimation of the cost for producing FeP was listed in Table S1 in the Supporting Information. Carbon cloth (CC) is a cheap textile with high conductivity and excellent flexibilility and strength[19] and the use of CC as support for catalysts also facilitates easier integration of the electrode into devices for applications. In this Letter, we report

Received: September 22, 2014
Accepted: November 17, 2014

   dx.doi.org/10.1021/am5064684 | ACS Appl. Mater. Interfaces XXXX, XXX, XXX−XXX

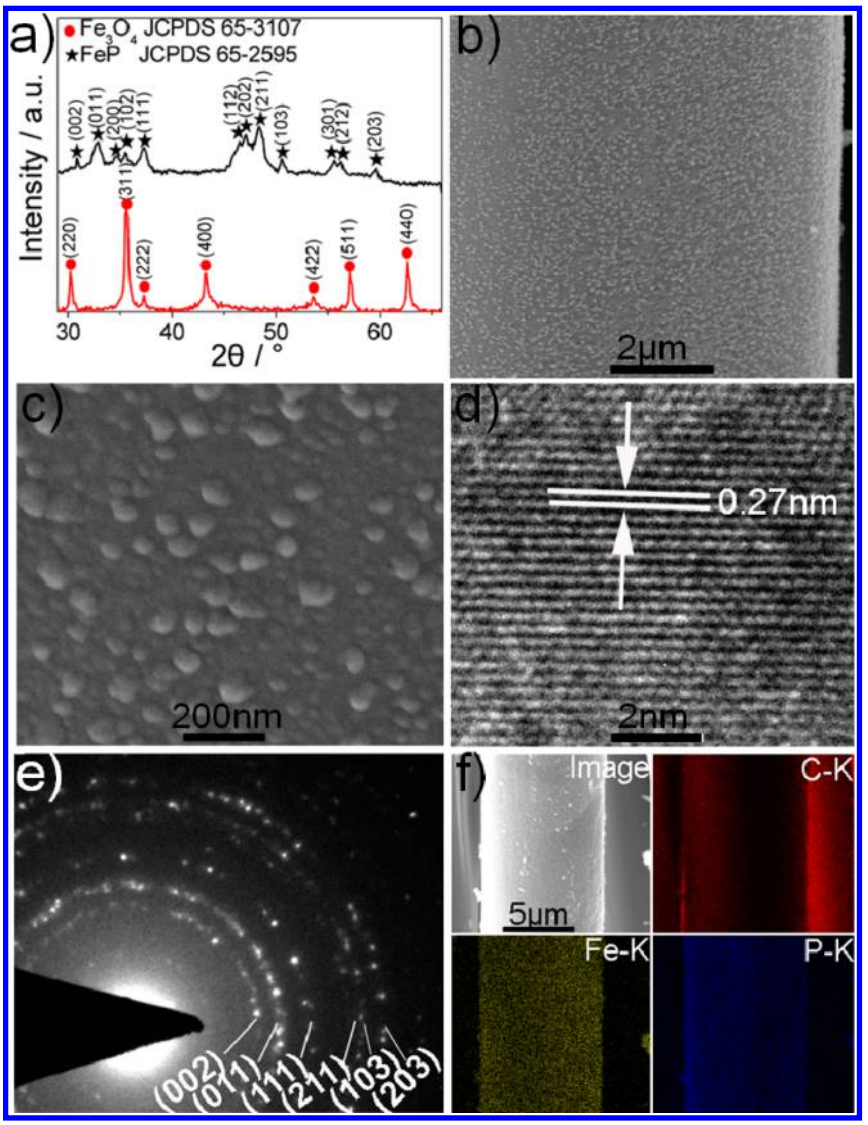

Figure 1. (a) XRD patterns for Fe_3O_4 and FeP. (b) Low- and (c) high-magnification SEM images of FeP/CC. (d) HRTEM image and (e) SAED pattern of FeP nanoparticles. (f) STEM image and EDX elemental mapping of C, Fe, and P for the FeP/CC.

that FeP nanoparticles film directly grown on CC (FeP/CC) can function as an ultrahighly active 3D hydrogen evolution cathode with catalytic power superior to previous FeP catalysts[16−18] and comparable to commercial Pt/C as well as good durability in acidic media. This electrode exhibits a low onset overpotential of 19 mV, a small Tafel slope of 32 mV dec^{-1}, and nearly 100% Faradaic efficiency (FE). It exhibits a large exchange current density of 0.59 mA cm^{-2} and can afford current densities of 20 and 100 mA cm^{-2} at overpotentials of 54 and 108 mV, respectively. It also works well under neutral conditions.

Figure 1a shows the X-ray diffraction (XRD) patterns for the precursor and its phosphided product scratched down from CC. The precursor shows diffraction peaks characteristic of Fe_3O_4 (JCPDS No. 65−3107) while only peaks corresponding to FeP phase (JCPDS No. 65−2595) occur for the phosphided product, confirming successful conversion of Fe_3O_4 into FeP after the low-temperature phosphidation reaction. The scanning electron microscopy (SEM) images of Fe_3O_4/CC precursor (see Figure S1 in the Supporting Information) show that the surface of CC is covered by continuous film of dense Fe_3O_4 nanoparticles having diameters of several tens of nanometers. After phosphidation, the integrated feature of the resulting FeP nanoparticles film and CC is still preserved (Figure 1b, c). The energy-dispersive X-ray (EDX) spectrum (see Figure S2 in the Supporting Information) shows that the atomic ratio of Fe/P is close to 1:1. The high-resolution transmission electron microscopy (HRTEM) image of the FeP nanoparticles reveals well-resolved lattice fringes with an interplanar distance of 0.27 nm corresponding to the (011) plane of FeP,[20] as shown in Figure 1d. The selected area electron diffraction (SAED) pattern (Figure 1e) shows diffraction rings with d values of 2.896, 2.729, 2.415, 1.880, 1.809, and 1.547 Å indexed to the (002), (011), (111), (211), (103), and (203) planes of FeP structure, respectively. The scanning TEM (STEM) image and corresponding EDX elemental mapping of C, Fe, and P for the FeP/CC (Figure 1f) further suggest the uniform distribution of both Fe and P elements in the FeP nanoparticles film grown on CC. All these experimental observations clearly confirm the formation of FeP/CC derived from Fe_3O_4/CC. It should be pointed out that the same preparation with the use of rigid graphite rod (GR) as support leads to crack-rich Fe_3O_4 and FeP nanoparticles films (Fe_3O_4/GR and FeP/GR), as shown in Figure S3 in the

dx.doi.org/10.1021/am5064684 | ACS Appl. Mater. Interfaces XXXX, XXX, XXX−XXX

Supporting Information. It suggests flexible support may favor the growth of continuous nanoparticles film, which may be attributed to that the highly textured surface of the carbon fiber facilitates the nucleation and growth of the catalyst layer with strong mechanical interaction.[21]

The electrocatalytic activity of FeP/CC (FeP loading: 4.2 mg cm^{-2}) was evaluated in 0.5 M H_2SO_4. For comparison study, we also tested blank CC and GR, FeP/GR (FeP loading: 4.1 mg cm^{-2}) and commercial Pt/C (20 wt % Pt/XC-72) loaded on CC (loading: 3.7 mg cm^{-2}). A resistance test was made and *iR* correction was applied to all electrochemical measurements (see Figure S4 in the Supporting Information). Five individual FeP/CC electrodes were tested and each electrode was measured three times and all results are quite reproducible. Figure 2a shows the polarization curves. Blank CC and GR

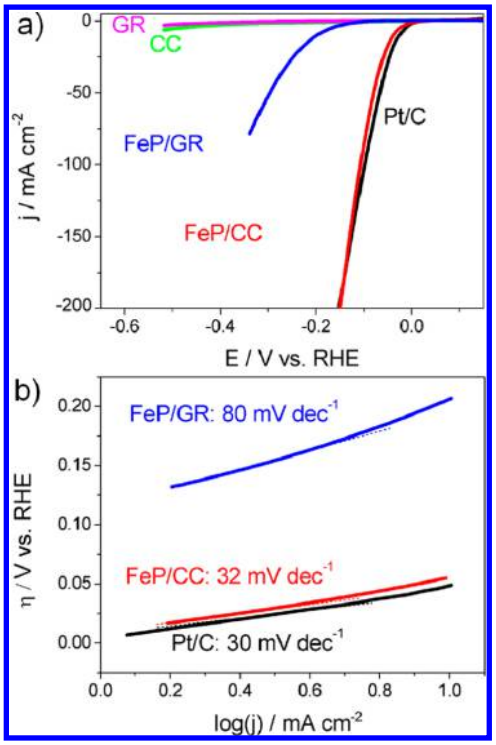

Figure 2. (a) Polarization curves of blank CC and GR, FeP/CC, FeP/GR, and Pt/C in 0.5 M H_2SO_4 at a scan rate of 2 mV/s. (b) Tafel plots for FeP/CC, FeP/GR, and Pt/C.

show negligible HER activities in the measurement voltage range. In contrast, the FeP/CC electrode shows a small onset overpotential of 19 mV, very close to the thermodynamic potential of HER (0 V) and much smaller than that of the FeP/GR electrode (135 mV). Moreover, this electrode affords current densities of 20 and 100 mA cm^{-2} at overpotentials of 54 and 108 mV, respectively. These overpotentials compare favorably to the behaviors of other FeP catalysts[16−18] and are almost comparable to the values needed by Pt/C.

FeP/GR shows a large Tafel slope of 80 mV dec^{-1} while FeP/CC gives a Tafel slope as low as 32 mV dec^{-1} (Figure 2b), suggesting superior catalytic activity of FeP/CC over FeP/GR. Obviously, the HER occurs on FeP/CC through a Volmer−Tafel mechanism with the Tafel reaction as the rate-determining step, which is similar to the HER mechanism on Pt (Tafel slope = 30 mV dec^{-1}).[22] Overall, the unexpectedly high catalytic activity and low price of the FeP/CC make it a promising hydrogen evolution cathode with highest performance-price ratio for large-scale electrochemical hydrogen production in acidic water (see Table S2 in the Supporting Information). Note that the evolved hydrogen gas as tiny bubbles efficiently escapes from the electrolyte at the electrode (see Movie S1 in the Supporting Information), which suppresses the loss in available surface area blocked by hydrogen and is a desired property for practical application. The exchange current density (j_0) of FeP/CC was calculated to be ~0.59 mA cm^{-2} by extrapolating the Tafel plot (see Figure S5 in the Supporting Information), which is 16 times of that for FeP/GR (~0.037 mA cm^{-2}) and the largest among the non-Pt catalysts listed in Table S2 in the Supporting Information.

The much superior catalytic activity of FeP/CC to FeP/GR can be rationally explained as follows. (1) The use of flexible conductive CC as substrate favors the formation of compact continuous film of FeP nanoparticles. It ensures intimate contact, good mechanical adhesion and excellent electrical connection among neighboring FeP as well as between FeP and CC, leading to enhanced electrons flowing from CC to FeP and through the whole nanoparticles film. (2) Electrochemical impedance spectroscopy analysis (see Figure S4 in the Supporting Information) shows that FeP/CC exhibits lower impedance and thus markedly faster HER kinetics than FeP/GR.[23] It is also worth mentioning that the FeP/CC exhibits much higher catalytic activity than previously reported FeP-GS catalyst.[17] It can be attributed to that the absence of polymer binder for FeP/CC not only leads to improved conductivity (see Figure S4 in the Supporting Information), but effectively avoids the block of active sites and the inhibition of diffusion.[13]

We performed accelerated degradation studies to probe the stability of the FeP/CC during repeated cycling in acidic environments. As shown in Figure 3a, the polarization curve shows a slight decay after the first 2000 cycles but remains unchanged until 5000 cycles in 0.5 M H_2SO_4 at a scan rate of 100 mV s^{-1}. The durability of the Pt/C/CC during repeated cycling in acidic environments was also investigated (Figure 3a inset). The polarization curve shows a larger decay after the first 2000 cycles compared with that of FeP/CC, and exhibits further decay in the following 3000 cycles. The interior durability of Pt/C/CC can be attributed to the weak mechanical adhesion between the Pt/C and CC, leading to the falling of some Pt/C nanoparticles from CC during the collapse of bubbles. The durability of FeP/CC was further measured by galvanostatic measurements at a cathodic current density of 50 mA cm^{-2} (Figure 3b). Negligible change in potential over 60 h of continuous operation was observed. Note that the FeP/CC exhibits superior durability over polypyrrole/MoS_x (PPy/MoS_x), which is the only previously reported Pt-free HER catalyst with performance comparable to commercial Pt/C.[22] Our FeP/CC has an additional advantage to PPy/MoS_x in that it is much more cost-effective. Thus, FeP/CC holds greater application potential than PPy/MoS_x. We also determined the Faradaic efficiency (FE) of the FeP/CC electrode for hydrogen evolution at pH 0 according to previously reported method.[8,11,14,15,18] The agreement of the amount of experimentally quantified hydrogen with theoretically calculated hydrogen (assuming 100% FE) suggests that the FE is close to 100%, as shown in Figure 3c.

Notably, the FeP/CC electrode also works efficiently in neutral solutions. Figure 4a shows the polarization curves for FeP/CC before and after 1000 CV cycles at a scan rate of 2 mV/s in 1.0 M phosphate buffer solution (PBS, pH 7),

dx.doi.org/10.1021/am5064684 | ACS Appl. Mater. Interfaces XXXX, XXX, XXX−XXX

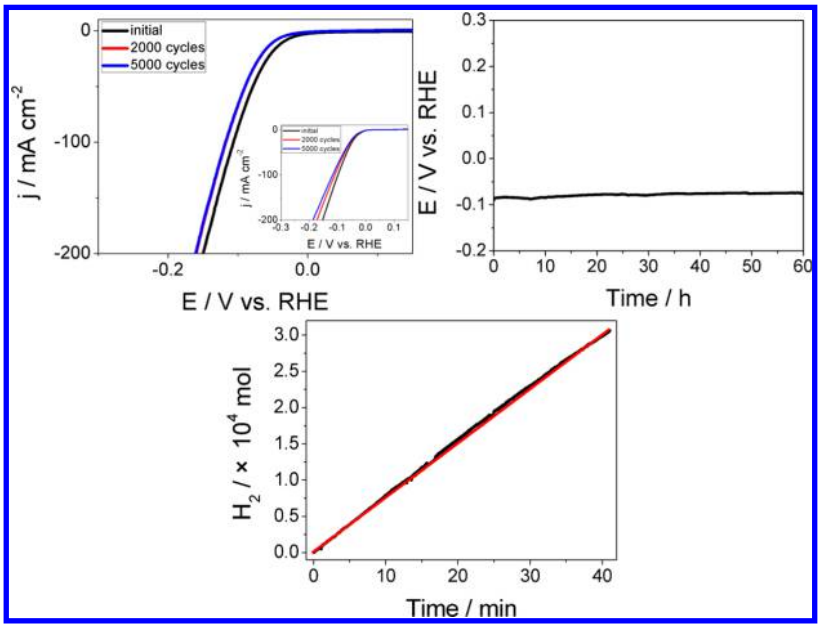

Figure 3. (a) Polarization curves for FeP/CC in 0.5 M H_2SO_4 initially and after 2000 and 5000 CV scans between +0.1 and −0.3 V vs RHE. Inset: Polarization curves for Pt/C/CC in 0.5 M H_2SO_4 initially and after 2000 and 5000 CV scans between +0.1 and −0.3 V vs RHE. (b) Time-dependent potential curve for FeP/CC under a constant cathodic current density of 50 mA cm^{-2} for 60 h. (c) Amount of H_2 theoretically calculated (red) and experimentally measured (black) versus time for FeP/CC in 0.5 M H_2SO_4.

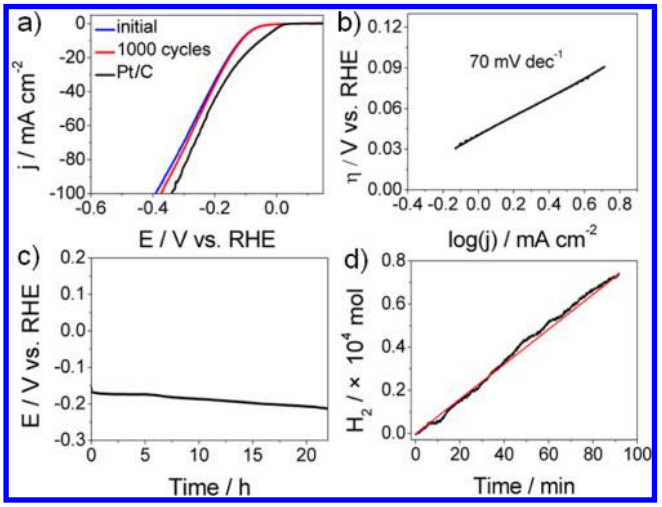

Figure 4. (a) Polarization curves for FeP/CC and Pt/C in 1.0 M PBS (pH 7) with a scan rate of 2 mV/s. (b) Tafel plot for FeP/CC. (c) Time-dependent potential curve for FeP/CC under a constant cathodic current density of 20 mA cm^{-2} for 22 h. (d) Amount of H_2 theoretically calculated (red) and experimentally measured (black) versus time for FeP/CC in 1.0 M PBS.

suggesting an onset overpotential of 46 mV and no measurable loss of catalytic activity. It shows a Tafel slope of 70 mV dec^{-1} (Figure 4b). To afford current density of 2 mA cm^{-2}, it needs an overpotential of 60 mV, which is the lowest among the values required by other non-noble metal HER catalysts in neutral solutions (see Table S3 in the Supporting Information). Galvanostatic measurement at a cathodic current density of 20 mA cm^{-2} was carried out for 22 h to evaluate the durability of FeP/CC under neutral conditions. As shown in Figure 4c, FeP/CC well-retains its HER activity and only exhibits a 40 mV decay in potential. We further measured the concentration of iron ions by ICP-MS in the electrolyte after electrolysis. It suggests that about 1.2% of the FeP catalyst was potentially removed from CC, suggesting the occurrence of some corrosion. In addition, this electrode also shows nearly 100% FE for hydrogen evolution at pH 7 (Figure 4d).

Figure S6a and S6b in the Supporting Information show the X-ray photoelectron spectroscopy (XPS) spectra of the Fe 2p and P 2p regions for FeP nanoparticles. The Fe $2p_{3/2}$ peaks appear at 707.7 and 712.0 eV and the Fe $2p_{1/2}$ peak appears at 720.2 eV. The high-resolution P(2p) region shows two peaks at 130.3 and 129.6 eV corresponding to P $2p_{1/2}$ and P $2p_{3/2}$, respectively, along with one peak at 134.2 eV. The peaks at 707.7 and 129.6 eV are close to the binding energies (BEs) for Fe and P in FeP.[24] The peaks at 720.2 and 134.2 eV can be assigned to oxidized Fe and P species stemming from superficial oxidation caused by exposure to air.[25] The existence of oxygen can be confirmed by the survey spectrum (see Figure S6c in the Supporting Information) and EDX spectrum (see Figure S2 in the Supporting Information). The Fe 2p BE (707.7 eV) is positively shifted from that of metallic Fe (706.8 eV) while the P 2p BE (129.6 eV) is negatively shifted from that of elemental P (130.2 eV).[25] It suggests that Fe and P in FeP carries a partial positive (δ^+) and negative (δ^-) charge, respectively,[26] which results from electron transfer from Fe to P.[24,25] Our recent work also demonstrate that CoP,[8,11] Cu_3P,[14] Ni_2P,[15] and MoP[27] as efficient HER catalysts feature pendant base P positioned close to the metal center. The active sites for hydrogenase also feature pendant bases proximate to the metal centers[28] and metal complex HER catalysts incorporate proton relays from pendant acid−base groups positioned close to the metal center where hydrogen evolution occurs.[29] It is believed that the Fe and P in FeP act as the hydride-acceptor and proton-acceptor center, respectively, which facilitates the HER.[9] In addition, the P could also facilitate the formation of Fe-hydride for subsequent hydrogen evolution via electrochemical desorption.[30]

In summary, our current work presents the first artificial Fe-based hydrogen evolution cathode with high activity comparable to that of commercial Pt/C and good durability in

dx.doi.org/10.1021/am5064684 | ACS Appl. Mater. Interfaces XXXX, XXX, XXX−XXX

strongly acidic media. This electrode also works well at neutral pH. The wide availability of Fe and carbon, the easy low-cost and scalable fabrication process and the high catalytic activity of this FeP/CC electrode place it as the most cost-effective and active 3D cathode toward electrochemical water splitting for large-scale hydrogen fuel production.

■ ASSOCIATED CONTENT

Supporting Information

Experimental details; SEM images; EDX and XPS spectra; XRD patterns; Tables S1−S3; calculation of exchange current density; Nyquist plots; Movie S1. This material is available free of charge via the Internet at http://pubs.acs.org.

■ AUTHOR INFORMATION

Corresponding Author

*E-mail: sunxp@ciac.ac.cn. Fax/Tel: (+86) 431-85262065.

Notes

The authors declare no competing financial interest.

■ ACKNOWLEDGMENTS

This work was supported by the National Natural Science Foundation of China (21175129) and the National Basic Research Program of China (2011CB935800).

■ REFERENCES

(1) Gray, H. B. Powering the Planet with Solar Fuel. *Nat. Chem.* **2009**, *1*, 7−7.

(2) Walter, M. G.; Warren, E. L.; McKone, J. R.; Boettcher, S. W.; Mi, Q.; Santori, E. A.; Lewis, N. S. Solar Water Splitting Cells. *Chem. Rev.* **2010**, *110*, 6446−6473.

(3) Hambourger, M.; Gervaldo, M.; Svedruzic, D.; King, P. W.; Gust, D.; Ghirardi, M.; Moore, A. L.; Moore, T. A. [FeFe]-Hydrogenase-Catalyzed H_2 Production in a Photoelectrochemical Biofuel Cell. *J. Am. Chem. Soc.* **2008**, *130*, 2015−2022.

(4) Kong, D.; Wang, H.; Cha, J. J.; Pasta, M.; Koski, K. J.; Yao, J.; Cui, Y. Synthesis of MoS_2 and $MoSe_2$ Films with Vertically Aligned Layers. *Nano Lett.* **2013**, *13*, 1341−1347.

(5) Vrubel, H.; Hu, X. Molybdenum Boride and Carbide Catalyze Hydrogen Evolution in both Acidic and Basic Solutions. *Angew. Chem., Int. Ed.* **2012**, *51*, 12703−12706.

(6) Cao, B.; Veith, G. M.; Neuefeind, J. C.; Adzic, R. R.; Khalifah, P. G. Mixed Close-Packed Cobalt Molybdenum Nitrides as Non-noble Metal Electrocatalysts for the Hydrogen Evolution Reaction. *J. Am. Chem. Soc.* **2013**, *135*, 19186−19192.

(7) Kundu, A.; Sahu, J. N.; Redzwan, G.; Hashim, M. A. An Overview of Cathode Material and Catalysts Suitable for Generating Hydrogen in Microbial Electrolysis Cell. *Int. J. Hydrogen Energy* **2013**, *38*, 1745−1757.

(8) Tian, J.; Liu, Q.; Asiri, A. M.; Sun, X. Self-Supported Nanoporous Cobalt Phosphide Nanowire Arrays: An Efficient 3D Hydrogen-Evolving Cathode over the Wide Range of pH 0−14. *J. Am. Chem. Soc.* **2014**, *136*, 7587−7590.

(9) Carenco, S.; Portehault, D.; Boissière, C.; Mèzailles, N.; Sanchez, C. Nanoscaled Metal Borides and Phosphides: Recent Developments and Perspectives. *Chem. Rev.* **2013**, *113*, 7981−8065.

(10) Popczun, E. J.; McKone, J. R.; Read, C. G.; Biacchi, A. J.; Wiltrout, A. M.; Lewis, N. S.; Schaak, R. E. Nanostructured Nickel Phosphide as an Electrocatalyst for the Hydrogen Evolution Reaction. *J. Am. Chem. Soc.* **2013**, *135*, 9267−9270.

(11) Liu, Q.; Tian, J.; Cui, W.; Jiang, P.; Cheng, N.; Asiri, A. M.; Sun, X. Carbon Nanotubes Decorated with CoP Nanocrystals: A Highly Active Non-Noble-Metal Nanohybrid Electrocatalyst for Hydrogen Evolution. *Angew. Chem., Int. Ed.* **2014**, *53*, 6710−6714.

(12) Luo, Y.; Jiang, J.; Zhou, W.; Yang, H.; Luo, J.; Qi, X.; Zhang, H.; Denis, Y.; Li, C. M.; Yu, T. Self-Assembly of Well-Ordered Whisker-Like Manganese Oxide Arrays on Carbon Fiber Paper and Its Application as Electrode Material for Supercapacitors. *J. Mater. Chem.* **2012**, *22*, 8634−8640.

(13) Roy-Mayhew, J. D.; Boschloo, G.; Hagfeldt, A.; Aksay, I. A. Functionalized Graphene Sheets as a Versatile Replacement for Platinum in Dye-Sensitized Solar Cells. *ACS Appl. Mater. Interfaces* **2012**, *4*, 2794−2800.

(14) Tian, J.; Liu, Q.; Cheng, N.; Asiri, A. M.; Sun, X. Self-Supported Cu_3P Nanowire Arrays as an Integrated High-Performance Three-Dimensional Cathode for Generating Hydrogen from Water. *Angew. Chem., Int. Ed.* **2014**, *53*, 9577−9581.

(15) Pu, Z.; Liu, Q.; Tang, C.; Asiri, A. M.; Sun, X. Ni_2P Nanoparticle Films Supported on a Ti Plate as an Efficient Hydrogen Evolution Cathode. *Nanoscale* **2014**, *6*, 11031−11034.

(16) Xu, Y.; Wu, R.; Zhang, J.; Shi, Y.; Zhang, B. Anion-Exchange Synthesis of Nanoporous FeP Nanosheets as Electrocatalysts for Hydrogen Evolution Reaction. *Chem. Commun.* **2013**, *49*, 6656−6658.

(17) Zhang, Z.; Lu, B.; Hao, J.; Yang, W.; Tang, J. FeP Nanoparticles Grown on Graphene Sheets as Highly Active Non-Precious-Metal Electrocatalysts for Hydrogen Evolution Reaction. *Chem. Commun.* **2014**, *50*, 11554−11557.

(18) Jiang, P.; Liu, Q.; Liang, Y.; Tian, J.; Asiri, A. M.; Sun, X. A Cost-Effective 3D Hydrogen Evolution Cathode with Exceptionally High Catalytic Activity: FeP Nanowire Array as the Active Phase. *Angew. Chem., Int. Ed.* **2014**, *53*, f12855−12859.

(19) Wang, G.; Wang, H.; Lu, X.; Ling, Y.; Yu, M.; Zhai, T.; Tong, Y.; Li, Y. Solid-State Supercapacitor Based on Activated Carbon Cloths Exhibits Excellent Rate Capability. *Adv. Mater.* **2014**, *26*, 2676−2682.

(20) Qian, C.; Kim, F.; Ma, L.; Tsui, F.; Yang, P.; Liu, J. Solution-Phase Synthesis of Single-Crystalline Iron Phosphide Nanorods/Nanowires. *J. Am. Chem. Soc.* **2004**, *126*, 1195−1198.

(21) Kong, D.; Wang, H.; Lu, Z.; Cui, Y. $CoSe_2$ Nanoparticles Grown on Carbon Fiber Paper: An Efficient and Stable Electrocatalyst for Hydrogen Evolution Reaction. *J. Am. Chem. Soc.* **2014**, *136*, 4897−4900.

(22) Wang, T.; Zhuo, J.; Du, K.; Chen, B.; Zhu, Z.; Shao, Y.; Li, M. Electrochemically Fabricated Polypyrrole and MoSx Copolymer Films as a Highly Active Hydrogen Evolution Electrocatalyst. *Adv. Mater.* **2014**, *26*, 3761−3766.

(23) Guo, C.; Zhang, L.; Miao, J.; Zhang, J.; Li, C. M. DNA-Functionalized Graphene to Guide Growth of Highly Active Pd Nanocrystals as Efficient Electrocatalyst for Direct Formic Acid Fuel Cells. *Adv. Energy Mater.* **2013**, *3*, 167−171.

(24) Grosvenor, A. P.; Wik, S. D.; Cavell, R. G.; Mar, A. Examination of the Bonding in Binary Transition-Metal Monophosphides MP (M = Cr, Mn, Fe, Co) by X-Ray Photoelectron Spectroscopy. *Inorg. Chem.* **2005**, *44*, 8988−8998.

(25) Li, L.; Chen, C.; Chen, L.; Zhu, Z.; Hu, J. Catalytic Decomposition of Toxic Chemicals Over Iron Group Metals Supported on Carbon Nanotubes. *Environ. Sci. Technol.* **2014**, *48*, 3372−3377.

(26) Rajesh, B.; Sasirekha, N.; Lee, S.; Kuo, H.; Chen, Y. Investigation of Fe−P−B Ultrafine Amorphous Nanomaterials: Influence of Synthesis Parameters on Physicochemical and Catalytic Properties. *J. Mol. Catal. A: Chem.* **2008**, *289*, 69−75.

(27) Xing, Z.; Liu, Q.; Asiri, A. M.; Sun, X. Closely Interconnected Network of Molybdenum Phosphide Nanoparticles: A Highly Efficient Electrocatalyst for Generating Hydrogen from Water. *Adv. Mater.* **2014**, *26*, 5702−5707.

(28) Nicolet, Y.; Piras, C.; Legrand, P.; Hatchikian, C.; Fontecilla-Camps, J. C. Desulfovibrio Desulfuricans Iron Hydrogenase: the Structure Shows Unusual Coordination to an Active Site Fe Binuclear Center. *Structure* **1999**, *7*, 13−23.

(29) Wilson, A. D.; Newell, R. H.; McNevin, M. J.; Muckerman, J. T.; Dubois, M. R.; Dubois, D. L. Hydrogen Oxidation and Production Using Nickel-Based Molecular Catalysts with Positioned Proton Relays. *J. Am. Chem. Soc.* **2006**, *128*, 358−366.

(30) Zhang, W.; Hong, J.; Zheng, J.; Huang, Z.; Zhou, J.; Xu, R. Nickel-Thiolate Complex Catalyst Assembled in One Step in Water for Solar H_2 Production. *J. Am. Chem. Soc.* **2011**, *133*, 20680−20683.